Paper No. 372. (quote when citing this article)
Eleventh World Conference on Earthquake Engineering
ISBN: 0 08 042822 3

ANALYSIS OF SITE LIQUEFACTION AND REMEDIATION

E. PARRA, K. ADALIER, A.-W. ELGAMAL, A. RAGHEB and M. ZEGHAL

Rensselaer Polytechnic Institute, Department of Civil Engineering
Troy, NY 12180, USA

ABSTRACT

A computational model for dynamically induced liquefaction is calibrated by centrifuge model tests. The model is a time domain code based on a nonlinear coupled solid-fluid formulation. Special attention is dedicated to the concept of cyclic mobility during liquefaction in dense granular soils. The effect of this dilation-induced phenomenon and the associated increase in soil stiffness is studied within the framework of remediation of an infinite-slope loose-sand site.

KEYWORDS

Site, amplification, soil, liquefaction, cyclic mobility, dilation.

INTRODUCTION

Recent major seismic events such as the 1989 Loma Prieta and the 1995 Hyogoken-Nanbu earthquakes continue to demonstrate the damaging effects of liquefaction-induced loss of soil strength and associated lateral spreading (Seed *et al.* 1990, Bardet *et al.* 1995). Experimental laboratory research on soil liquefaction and analysis of field instrumentation has provided valuable insight concerning excess pore-pressure buildup (National Research Council 1985). However, for engineering applications, there remains a need to further understand and identify the mechanisms of seismically induced soil deformation due to liquefaction, and related stiffness and strength degradation.

Centrifuge model tests provide a valuable source of information about the mechanisms of liquefaction and lateral spreading. In this regard, the VELACS (Verification of Liquefaction Analysis by Centrifuge Studies) project is unique (Arulanandan and Scott 1993, 1994). Within this project, tests were conducted on ten saturated soil (and soil-structure) centrifuge models with well defined boundary conditions, soil properties, and input dynamic motions. The recorded experimental data included accelerations, displacements, settlements and excess pore pressure histories.

In this paper, a computational model for soil liquefaction was calibrated by experimental laboratory data, and by centrifuge tests conducted at Rensselaer Polytechnic Institute. In the following sections, the data employed for calibration is discussed, and the computational model is presented. This model is then used to study, in plane-strain, the response of an infinite slope with and without a liquefaction countermeasure to resist lateral

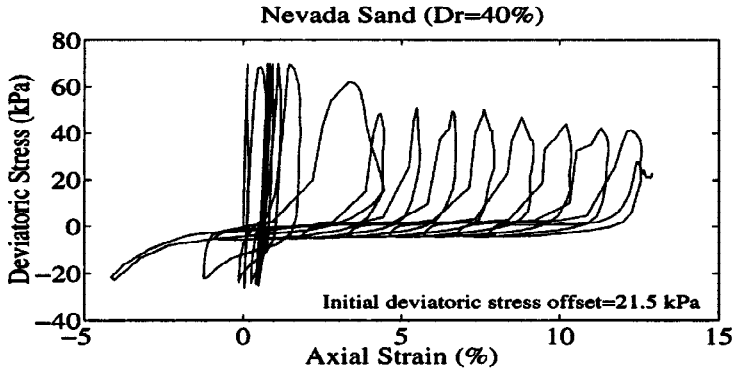

Fig. 1 Stress-strain history of a Nevada sand sample at $D_r = 40\%$, subjected to an undrained stress-controlled cyclic triaxial test and stress bias (after Arulmoli 1992).

deformations. Remediation is based on the following concepts: 1) increased stiffness in densified zones (sand columns), 2) increased drainage (wick drain effect, Seed and Booker 1977), and 3) the combined effect of stiffness and drainage (gravel or stone columns).

SOIL PROPERTIES

The liquefiable material properties were patterned after those of Nevada sand with a relative density (D_r) in the range of 40%. This sand was thoroughly tested under cyclic loading conditions by Arulmoli *et al.* 1992. For the purposes of this study, the most important feature of observed laboratory response is depicted in Fig. 1. As may be noted, the process of asymmetric cyclic shear loading during liquefaction has resulted in a cycle by cycle accumulation of shear strains; and has clearly displayed a process of regain in stiffness and strength at the large shear strain cyclic excursions. This pattern of response limits the amount of deformation during each loading cycle (Castro 1975, Zeghal and Elgamal 1994). The same response was clearly observed in a series of insightful centrifuge tests conducted at RPI (Taboada and Dobry 1993, Dobry and Taboada 1994, Taboada 1995). In these tests, dynamic centrifuge experiments on a Nevada sand stratum in an inclined laminated (Van Laak *et al.* 1994) container, documented the same pattern of regain in stiffness at large shear strain excursions (Taboada 1995, Elgamal *et al.* 1996). As will be shown below, the constitutive model employed herein was developed to mimic the above described cyclic loading behavior; so as to provide reliable estimates of liquefaction-induced cyclic deformations.

CONSTITUTIVE MODEL AND NUMERICAL IMPLEMENTATION

An effective-stress finite element (FE) algorithm has been developed to predict dynamic soil response (Ragheb 1994, Parra 1996). This algorithm is based on a two phase solid-fluid u-p formulation (Biot 1962, Zienkiewicz *et al.* 1990, Chan 1988). Soil skeleton constitutive behavior was represented using a newly-developed multi-surface plasticity model (Parra 1996), which was calibrated by laboratory data (Arulmoli *et al.* 1992) and by centrifuge testing results conducted by Taboada and Dobry 1993, and Taboada 1995. The salient features of this model are presented in Appendix I.

COMPUTATIONAL MODELLING OF LATERAL DEFORMATION

The response of an infinite mildly sloping stratum of saturated Nevada sand was studied. The stratum is 10 m in depth, and is inclined at a slope of 5 degrees to the vertical (Fig. 2). A shear beam response was mimiced by connecting lateral boundary nodes on either side of the finite element mesh. Soil permeability was taken as $k = 6.6 \times 10^{-5}$ m/sec, at the 40% relative density. Saturated soil mass density was taken as $\rho = 1973$ kg/m^3, angle of

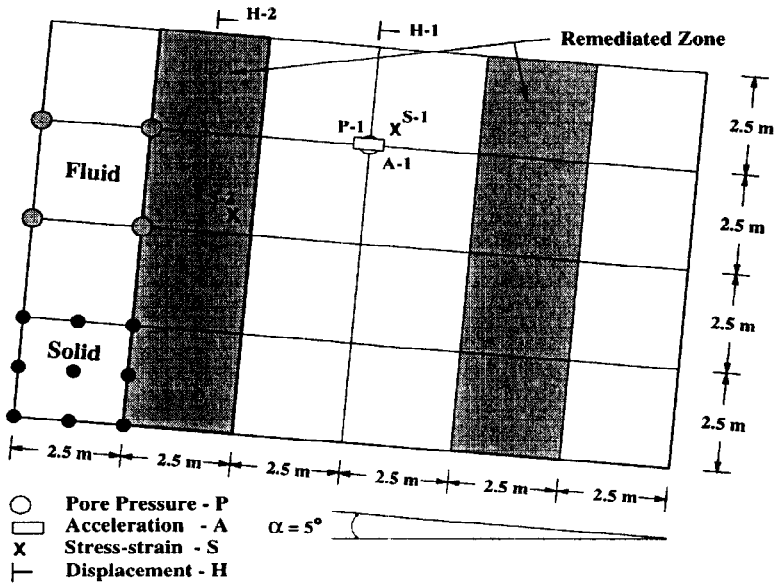

Fig. 2 Finite Element discretization of the infinite sloping stratum of saturated Nevada Sand and sampling locations.

internal friction $\phi = 32°$, phase transformation angle (*i.e.* the angle at which contractive and dilative zones are separated in the $p\prime - q$ space, Ishihara *et al.* 1975) $\phi_{pt} = 26.5°$. Low-strain shear modulus $G_o = 6.5 \times 10^4$ kPa at a reference confining pressure $p_r = 80$ kPa, and Poisson ratio $\nu = 0.42$. Finally, Low-strain moduli were considered to vary with the effective confining pressure at the power of $n = 0.5$.

This model was subjected to uniform cycles of harmonic base excitation (0.2 g peak amplitude), and the results are shown in Figs. 3-5. In view of the large shaking amplitudes, excess pore-pressures attained the vertical effective stress values indicating the occurrence of liquefaction (Fig. 3). However, the associated acceleration response did not vanish due to the reduction in pore-pressure and the associated regain in stiffness and strength at each cyclic large shear strain excursion (Fig. 4). Lateral permanent deformations at ground surface attained a total of 0.66 m at the end of dynamic excitation (Fig. 5).

Remediated ground

1) Remediation by increased drainage

In this case, the columns shown in Fig 2. were modelled as a draining material with the same frictional characteristics, but with an increased permeability of 1000 times that of Nevada sand. The computed results showed the following main response patterns: i) the lateral deformation at ground surface was reduced from 0.66 m to about 0.53 m (Fig. 5), ii) high drainage appeared to reduce the rate of pore pressure buildup within the draining material, but apparently had a small impact on pore-pressure buildup within the original sand. Even within the drain, it was observed that drainage mainly affected the upper zones near the free draining ground surface (Fig. 4a). Here, it may be concluded that drainage would have achieved better results if the high drainage columns were distributed more uniformly along the stratum lateral extent.

2) Remediation by increased stiffness

In this case, the constitutive model parameters were adjusted to model a dense Nevada sand ($D_r = 85\% - 90\%$) within the columns of Fig. 2. The computed results show a substantial reduction in accumulated strains within these dense zones (Fig. 4b); and a reduction in surface lateral deformations from 0.66 m to 0.40 m (Fig. 5). However, the original soil contained within the dense columns was found to liquefy, and accumulate large per-

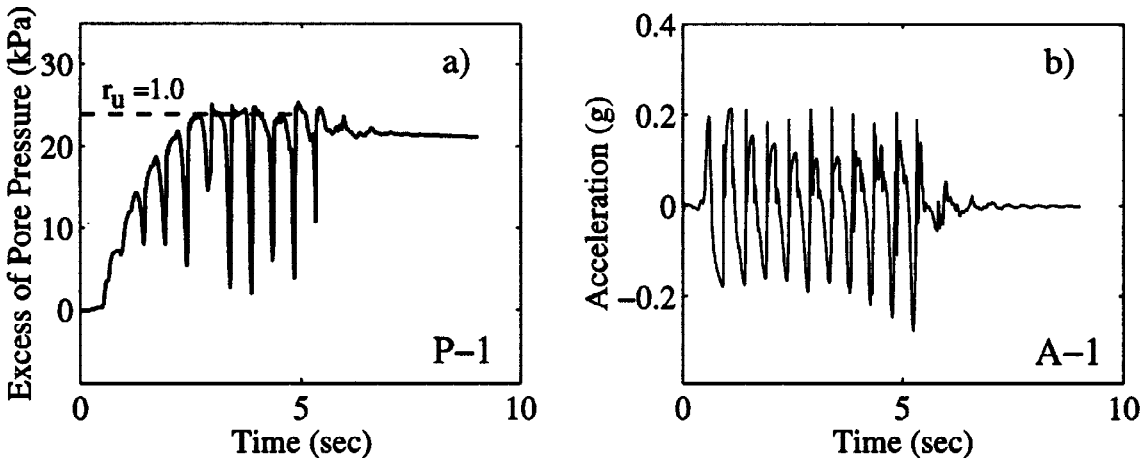

Fig. 3 (a) Excess pore pressure and (b) acceleration histories at the center of the FE mesh and at 2.5 m depth corresponding to no remediation configuration.

manent strains. Here, it may be concluded that the dense materials have supported the original loose material.

3) Remediation by drainage and increased stiffness

In this case, the columns of Fig. 2 were modeled to represent the stone column remediation technique. Such columns possess the high permeability, and high stiffness characteristics simultaneously. As may be observed from Fig. 5, the surface displacements were reduced to the lowest value of 0.23 m in permanent lateral deformation. Again, the main reason for this reduction in deformations stemed from the stiffness and strength of the introduced columns. Here, it was observed that the increased drainage had the following effects: i) faster pore-pressure dissipation, and ii) associated reduced tendency for dilation in the dense drain material, due to this high permeability (Fig. 4c and 4d). Nevertheless, the presence of increased permeability had a positive impact on controlling lateral deformations.

SUMMARY AND CONCLUSIONS

A computational model calibrated by laboratory and centrifuge testing data was employed to explore countermeasures against liquefaction-induced lateral deformations. Increased drainage was found to primarily contribute to increased strength within the high drainage remediated zones. Increased stiffness introduced by soil densification, or use of dense stone columns was more helpful in controlling the extent of lateral deformations, as the stiff material supported the surrounding loose liquefied zone.

ACKNOWLEDGMENTS

The research reported herein was supported by INTEVEP, SA, Venezuela, the National Science Foundation (grant No. MSS-9057388), and the National Center for Earthquake Engineering Research (grant No. 90-1503). This support is gratefully acknowledged.

APPENDIX I

Soil was modeled as a two phase material using the Biot (1962) formulation for porous media. This formulation was incorporated in a general purpose 2-D finite element program (Ragheb 1994, Parra 1996) using the u - p formulation (in which displacement of the soil skeleton, u, and pore pressures, p, are the unknowns) suggested by Zienkiewicz *et al.* (1990). The computational scheme follows the methodology of Chan (1988), which is

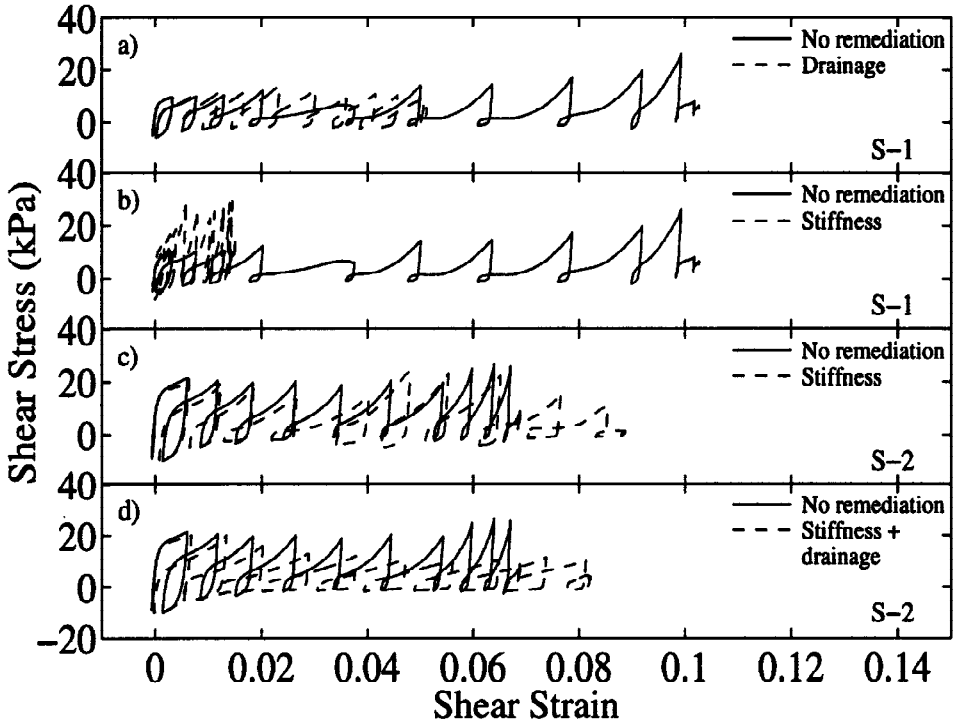

Fig. 4 Shear stress-strain histories sampled at: a) S-1 for increased drainage; b) S-1 for increased stiffness; c) S-3 for increased stiffness; and d) S-3 for increased stiffness and drainage.

based on the following assumptions: small deformations and rotations, density of the solid and fluid is constant in both time and space, porosity is locally homogeneous and constant with time, incompressibility of the soil grains, and equal accelerations for the solid and fluid phases. Therefore, the general coupled formulation after the spatial discretization and Galerkin approximation is expressed as follows:

$$\mathbf{M}\ddot{\mathbf{u}} + \int_{\Omega} \mathbf{B}^T \boldsymbol{\sigma}' \, d\Omega - \mathbf{Q}\,\bar{\mathbf{p}} - \mathbf{f}^S = \mathbf{0} \tag{1a}$$

$$\mathbf{G}\ddot{\mathbf{u}} + \mathbf{Q}^T \dot{\mathbf{u}} + \mathbf{H}\,\bar{\mathbf{p}} + \mathbf{S}\,\dot{\bar{\mathbf{p}}} - \mathbf{f}^p = \mathbf{0} \tag{1b}$$

where $\mathbf{M}$ is the mass matrix, $\mathbf{B}$ is the strain-displacement matrix, $\boldsymbol{\sigma}'$ is the effective stress vector, $\mathbf{Q}$ is the discrete gradient operator coupling the solid and fluid phases, $\bar{\mathbf{u}}$ is the displacement vector, $\bar{\mathbf{p}}$ is the pore pressure vector, $\mathbf{G}$ is the dynamic seepage force matrix, $\mathbf{H}$ is the permeability matrix, $\mathbf{S}$ is the compressibility matrix, and $\mathbf{f}^S$ and $\mathbf{f}^p$ are the prescribed boundary conditions for solid and fluid phase respectively. A superposed dot denotes time derivative. Viscous damping is added for the solid phase in the form of Rayleigh damping ($\mathbf{C} = \alpha\mathbf{M} + \beta\mathbf{K}$, where $\mathbf{K}$ is the initial stiffness matrix). For earthquake loading problems, $\mathbf{G}$ is usually neglected so that symmetry of the global matrix is attained.

Equation 1 is integrated in time using a simple single step predictor multi-corrector scheme of the Newmark type (Katona and Zienkiewicz 1985), with an automatic time stepping split algorithm, incorporated to improve the rate of convergence. The predictor is calculated using the initial stiffness matrix method, as the high degree of non-associativity shown in the behavior of the solid phase for granular materials, produces a non-symmetric tangent stiffness matrix that requires a non-symmetric matrix solver. Experience based on analyses of non-associative plasticity shows that the initial stiffness method performs reasonably well (Chan 1988).

The second term in Eq. 1a is defined by the soil constitutive model. In this study, a new model is developed and used, based on the original work on plasticity theory for frictional cohesionless soils (Prevost 1985). The new model (Parra 1996) provides flexibility in modeling the cyclic mobility phenomenon. Special attention is given to the way the deviatoric - volumetric strain coupling occurs under cyclic loading, especially for loading - unloading - reloading situations above the phase transformation line, and near the liquefaction condition

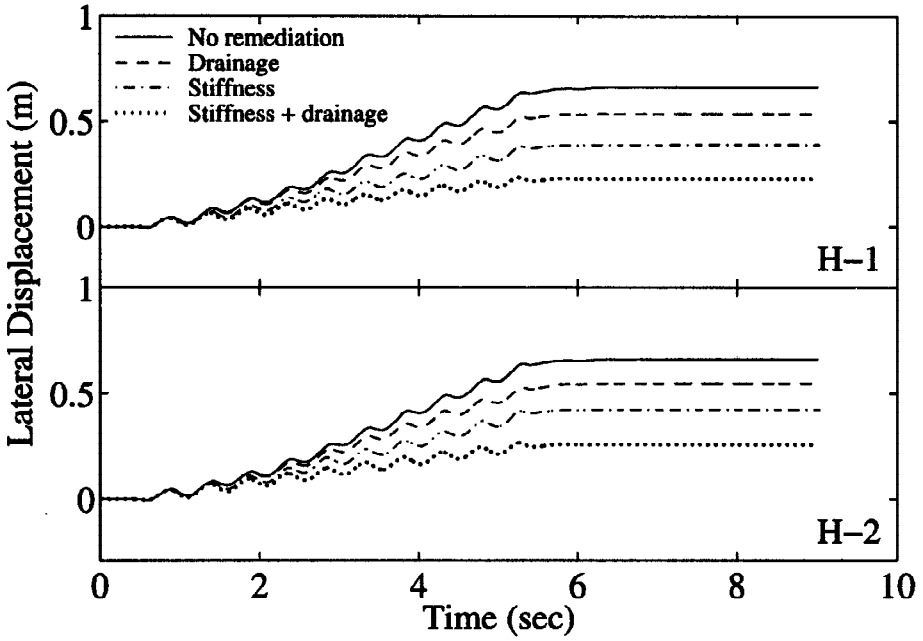

Fig. 5 Lateral displacement histories at H-1 and H-2 locations.

($p' = 0$ condition).

The constitutive equation is written in incremental form as follows (Prevost 1985):

$$\dot{\boldsymbol{\sigma}} = \mathbf{E} : (\dot{\boldsymbol{\epsilon}} - \dot{\boldsymbol{\epsilon}}^p) \tag{2}$$

where $\dot{\boldsymbol{\sigma}}$ is the rate of effective stress tensor, $\dot{\boldsymbol{\epsilon}}$ is the rate of deformation tensor, $\dot{\boldsymbol{\epsilon}}^p$ is the plastic rate of deformation tensor, and $\mathbf{E}$ is the isotropic elastic coefficient fourth order tensor. In this equation the superposed dot denotes a material derivative. The plastic rate of deformation tensor is defined by: $\dot{\boldsymbol{\epsilon}}^p = \mathbf{P}\ \langle L \rangle$, where $\mathbf{P}$ is a symmetric second-order tensor which defines the direction of plastic deformation in stress space, L is the plastic loading function; and the symbol $\langle\ \rangle$ denotes the McCauley's brackets (*viz.*, $L = 0$ if $L < 0$). Otherwise, L is defined as: $L = \mathbf{Q} : \dot{\boldsymbol{\sigma}}/H'$, where H' is the plastic modulus, and $\mathbf{Q}$ is a symmetric second-order tensor which defines, in stress space, the direction of the outer normal to the yield surface ($\mathbf{Q} = \nabla f / \|\nabla f\|$). The yield function, f, representing the states of stress for which plastic flow occurs, is selected as a family of nested cone surfaces connected at the apex as follows (Lacy 1986):

$$f = \frac{3}{2}(\mathbf{s} - \bar{p}\boldsymbol{\alpha}) : (\mathbf{s} - \bar{p}\boldsymbol{\alpha}) - m^2\bar{p}^2 = 0 \tag{3}$$

where $\mathbf{s} = \boldsymbol{\sigma} - \bar{p}\,\boldsymbol{\delta}$ is the deviatoric stress tensor, $\bar{p} = p - a$ with p and a representing the effective mean normal stress and the attraction at the apex (given by the amount of residual shear strength) respectively, $\boldsymbol{\alpha}$ is the kinematic deviatoric tensor defining the coordinates of the yield surface, and m is a material parameter to describe the friction angle ϕ.

The flow rule is chosen so that the deviatoric component of flow $\mathbf{P}' = \mathbf{Q}'$ (associative flow rule in the deviatoric plane), and the volumetric component P'' gives the desired amount of dilation or contraction in accordance with laboratory or field observations. Consequently, P'' defines the degree of non-associativity of the flow rule and is given as follows (Parra 1996):

$$3P'' = \frac{(\eta/\bar{\eta})^2 - 1}{(\eta/\bar{\eta})^2 + 1}\,\psi_d\ \langle \xi_d \rangle \tag{4}$$

where $\eta = \left(\frac{3}{2}\mathbf{s} : \mathbf{s}\right)^{1/2}/\bar{p}$ is effective stress ratio, $\bar{\eta}$ is a material parameter defining the stress ratio at the phase transformation (PT) line, ψ_d is a dilation function scaling the amount of dilation or contraction depending on

the level of confining pressure and cumulative plastic deformation, and $\xi_d = f\left(\varepsilon_d^p - \varepsilon_y^p\right)$ is an effective dilation function triggered at the point when the cumulative plastic deformation in the dilative zone (ε_d^p) reaches a predefined yielding level ε_y^p. Dilation or contraction is defined by the sign of $(\eta/\bar{\eta})^2 - 1$. If negative, the stress point lies below the PT line and contraction takes place. On the other hand, when the sign is positive the stress point lies above the PT line and dilation occurs. However, contrary to the original Prevost 1985 formulation, contraction above the PT line is performed towards the point where dilation started, which acts as a memory for the dilation-contraction condition. At the point of initial liquefaction or $p' = 0$ only dilation is allowed and upon contraction P'' is set equal to zero.

A purely deviatoric kinematic rule is chosen according to: $\bar{p}\dot{\alpha} = a\mu$, where μ is a deviatoric tensor defining the direction of translation (Lacy 1986) and a is the amount of translation dictated by the consistency condition.

The integration of the constitutive equations is performed using a stress point algorithm based upon the radial return method in the deviatoric plane (Lacy 1986), with an automatic strain stepping split algorithm which guarantees convergence and accuracy at all levels of strain (Parra 1996).

REFERENCES

Arulanandan, K. and Scott, R. F., eds. (1993). *Verification of Numerical Procedures for the Analysis of Soil Liquefaction Problems*, Conference Proceedings, Davis, CA, Volume **1**, Balkema.

Arulanandan, K. and Scott, R. F., eds. (1994). *Verification of Numerical Procedures for the Analysis of Soil Liquefaction Problems*, Conference Proceedings, Davis, CA, Volume **2**, Balkema.

Arulmoli, K., Muraleetharan, K. K., Hossain, M. M., and Fruth, L. S. (1992). *VELACS: Verification of Liquefaction Analyses by Centrifuge Studies, Laboratory Testing Program, Soil Data Report*, Report, The Earth Technology Corporation, Project No. 90-0562, Irvine, California.

Bardet, J. P., Oka, F., Sugito, M., and Yashima, A. (1995). *The Great Hanshin Earthquake Disaster, Prelim. Investigation Report*, Department of Civil Engineering, University of Southern California, Los Angeles, California.

Biot, M. A. (1962). The Mechanics of Deformation and Acoustic Propagation in Porous Media. *J. Appl. Phys.*, **33**, No. 4, 1482-1498.

Castro, G. (1975). Liquefaction and Cyclic Mobility of Saturated Sands. *Journal of the Geotechnical Engineering Division*, ASCE, **101**, No. GT6, 551-569.

Chan, A. H. C. (1988). A Unified Finite Element Solution to Static and Dynamic Problems in Geomechanics. *Ph.D. dissertation*, University College of Swansea, U. K.

Dobry, R. and Taboada, V. M. (1994). Possible Lessons from VELACS Model No. 2 Results, *Proceedings of the International Conference on the Verification of Numerical Procedures for the Analysis of Soil Liquefaction Problems*, Arulanandan, K. and Scott, R. F., eds., Volume **2**, Davis, CA, 1341-1352, Balkema.

Elgamal, A.-W., Zeghal, M., Taboada, V. M. and Dobry, R. (1996). Analysis of Site Liquefaction and Lateral Spreading using Centrifuge Model Tests. *Soils and Foundations*, (to appear)

Ishihara, K., Tatsuoka, F., and Yasuda, S. (1975) Undrained Deformation and Liquefaction of Sand under Cyclic Stresses. *Soils and Foundations*, **15**, No. 1, 29-44.

Katona, M. G. and Zienkiewicz, O. C. (1985). A Unified Set of Single Step Algorithms. Part 3: The Beta-m Method, A Generalization of the Newmark Scheme. *Int. J. Num. Meth. Engrg.*, **21**, 1345-1359.

Lacy, S. (1986). Numerical Procedures for Nonlinear Transient Analysis of Two-phase Soil System. *Ph.D. dissertation*, Princeton University, NJ, U.S.A.

National Research Council (1985). *Liquefaction of Soils During Earthquakes*, Committee on Earthquake Engineering, National Academy press, Washington D. C.

Parra, E. (1996). Numerical Modeling of Liquefaction and Lateral Ground Deformation Including Cyclic Mobility and Dilation Response in Soil System. *Ph.D. Thesis* in progress. Rensselaer Polytechnic Institute, Troy, NY.

Prevost, J. H., (1985). A Simple Plasticity Theory for Frictional Cohesionless Soils. *Soil Dyn. and Earthq. Eng.*, **4**, No. 1, 9-17.

Ragheb, A. (1994). Numerical analysis of Seismically Induced Deformations in Saturated Granular Soil Strata. *Ph.D. Thesis*, Rensselaer Polytechnic Institute, Troy, NY.

Seed, H. B. and Boocker, J. R. (1977). Stabilization of Potential Liquefiable Sand Deposits using Gravel Drains. *Journal of the Geotechnical Engineering Division*, ASCE, **103**, No. GT7, July, 757-768.

Seed, R. B., Dickenson, S. E., Riemer, M. F., Bray, J. D., Sitar, N., Mitchell, J. K., Idriss, I. M., Kayen, R. E., Kropp, A., Hander, L.F. Jr. and Power, M. S. (1990). *Preliminary Report on the Principal Geotechnical Aspects of the October 17, 1989, Loma Prieta Earthquake*, Report No. UCB/EERC-90/05, Earthquake Engineering Research Center, University of California Berkeley.

Taboada, V. M. (1995). Centrifuge Modeling of Earthquake-induced Lateral Spreading in Sand using a Laminar Box. *Ph.D. Thesis*, Rensselaer Polytechnic Institute, Troy, NY.

Taboada, V. M. and Dobry, R. (1993). Experimental Results of Model 1 at RPI, *Proceedings of the International Conference on the Verification of Numerical Procedures for the Analysis of Soil Liquefaction Problems*. Arulanandan, K. and Scott, R. F., eds., Volume **1**, Davis, CA, 277-294, Balkema.

Van Laak, P., Taboada, V., Dobry, R., and Elgamal, A.-W., (1994). Earthquake Centrifuge Modeling Using a Laminar Box, Dynamic Geotechnical Testing: Volume **II**, ASTM STP 1213, Ebelhar, R. J., Drnevich, V. P. and Kutter, B. L., eds. American Society of Testing Materials, Philadelphia.

Zeghal, M. and Elgamal, A.-W. (1994). Analysis of Site Liquefaction Using Earthquake Records, *Journal of Geotechnical Engineering*, ASCE, **120**, No. 6, 996-1017.

Zienkiewicz, O. C., Chan, A. H. C., Pastor, M., Paul, D. K., and Shiomi, T. (1990). Static and Dynamic Behaviour of Soils: A Rational Approach to Quantitative Solutions: I. Fully Saturated Problems. *Proc. R. Soc. Lond.*, **A 429**, 285-309.